TECHNICAL MEMORANDUM

Center for Multidisciplinary Research in Transportation
Texas Tech University
Lubbock, Texas 79409
806-742-3037 – FAX 806-742-3488

Date: 1/23/2023	**Study No:** 0000029807
To: Larry Blackburn, P.E.	**Tech Memo No:** Techmemo 0000029807-1
From: Research Team	**Revision No:**
Subject: **Evaluation of the Pavement Condition in FM 2094 in Houston**	

Table of Contents

Table of Figures

Introduction

A request was made under the inter-agency contract (IAC Contract No. 601CT0000029807) by the Houston District to conduct field testing and analyze data to identify the causes of distresses on FM 2094, as well as to provide recommendations on optimum rehabilitation strategies. The subject pavement on FM 2094 (CSJ: 0976-04-009) was completed in April 1992, and the pavement structure consists of 10-in CRCP + 1-in ASB + 6-in CTB + 6-in LTS (lime-treated subgrade). Accordingly, at the time of the field evaluation, the pavement was more than 30 years old.

The condition of the subject section was evaluated at the project site, and undulations on the pavement surface, longitudinal cracking and faulting were the major distresses observed. Those distress types are not typical observed in CRCP in Texas. Undulations on concrete slab surface occur only when there are volume changes taking place in primarily subgrade soil. Volume changes in subgrade soil also cause longitudinal cracking in CRCP.

In pavement design and construction, expansive or reactive soils pose major issues. Some clay minerals within reactive soils experience volume changes when exposed to changes in water content. This condition could lead to surface undulation of the concrete pavements, resulting in issues on serviceability and safety as well as distresses such as uncontrolled cracking.

To identify the causes of the pavement distresses observed in the subject project, field testing was conducted on December 20, 2022. The field testing conducted covered deflection testing with FWD from 29°32'20.35" N, 95°3'54.68" W up to is 29°32'8.35"N, 95° 4'4.68"W traversing about 1520-feet in length. In addition, coring, dynamic cone penetrometer (DCP) testing, and MIRA testing were also conducted. Soil samples were obtained from cored locations and various soil testing activities, including the Atterberg limits, moisture content and shrink-swell, were performed. Figure 1 illustrates the project location as well as the locations where 4 cores were taken. FWD testing was initially conducted to determine the deflections at regular intervals across the section. Subsequently, four (4) coring locations were identified, and core samples were extracted. DCP testing followed to estimate the modulus of the subgrade soil. Lastly, soil samples were extracted from the subgrade for laboratory testing of soil properties.

Figure 2 shows some of the sections with longitudinal cracking, faulting, undulations and resulting ponding of water. This has led to further deterioration of ride quality and pavement condition. Figures 3 to 8 show the coring, DCP and soil extraction activities conducted in the field. Based on all the information gathered, a recommended optimum rehabilitation strategy was developed.

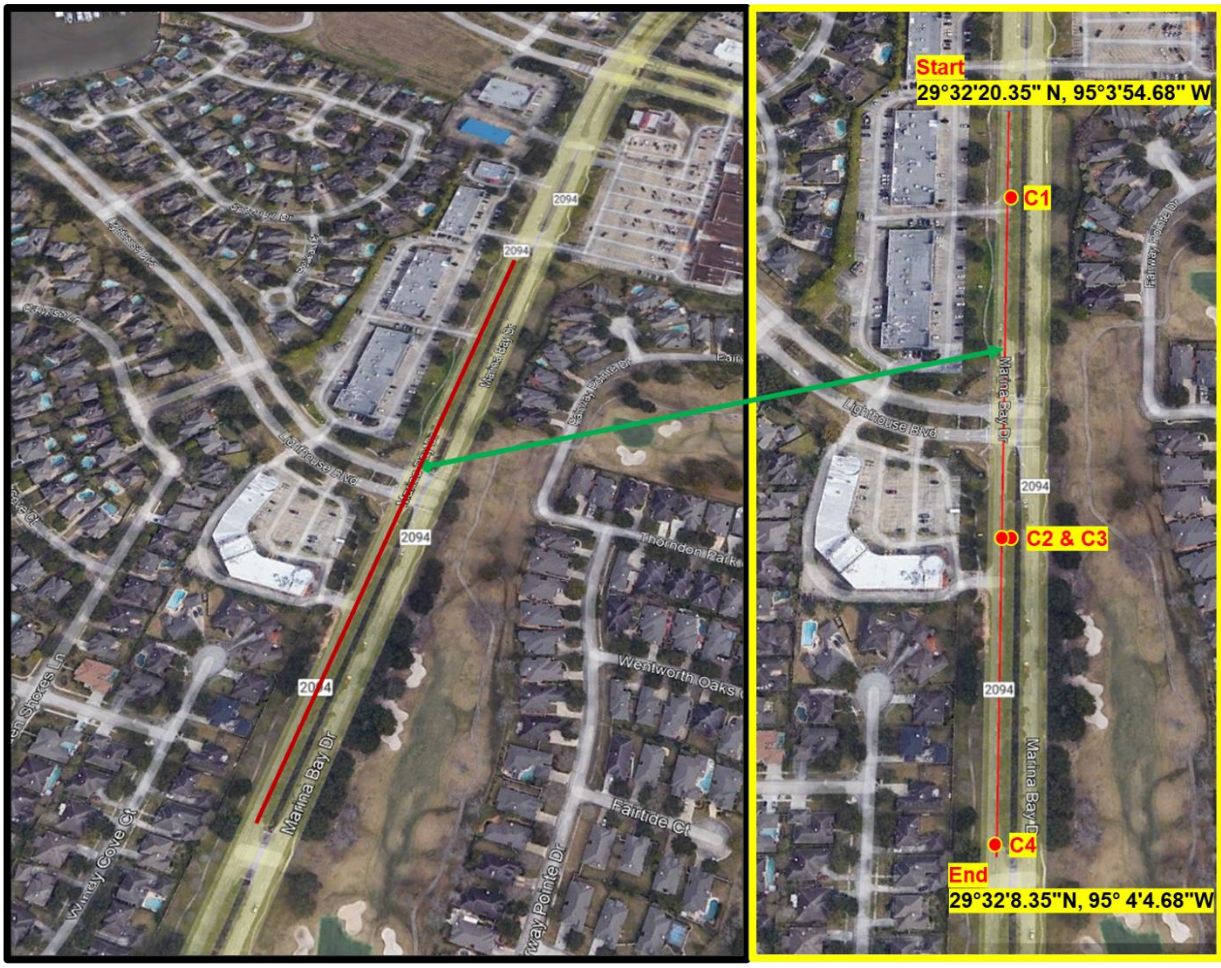

Figure 1 Field testing location

Figure 2 Distresses observed at the test section (Longitudinal cracking, faulting, and water ponding)

Figure 3 FWD testing at the test section.

Figure 4 Coring operation

Figure 5 Extracted core samples

Figure 6 DCP testing

Figure 7 Soil extraction

Figure 8 Investigation of the core location

The following sections present the results of the testing conducted during the field testing as well as the identification of the volume change potential of the subgrade soil. The structural capacity of the in-situ CRCP system evaluated by deflection testing as well as DCP testing is presented first, followed by the characteristics of the subgrade soil evaluated in the laboratory, and finally the presentation of rehabilitation options based on the test results.

Slab Deflections

Deflections on the CRCP slab were evaluated at the inside lane at every 20-ft. Figure 9 presents the deflections at 9,000-lb loading evaluated along the inside lane covering a total length of 1520-ft. It can be observed that the deflections were generally lower than 5 mils except for the specific DMI between 80–170 and 940–1460. The state-wide average of 10-in CRCP is about 2.5 mils, and it is observed that, even though the deflections obtained are comparable to the state-wide average value in some areas, in other areas, deflections are much larger, implying that voids exist in those areas, where longitudinal cracks were observed. Based on this deflection data, 4 locations were selected for further investigation with coring/DCP/soil extraction. The deflection in Core #1 was 6.04 mils whereas in Cores 2 and 3, at the same DMI, was 20.49 mils. Lastly, in Core 4, the deflection was 21.49 mils.

The visual distress survey has identified a longitudinal crack within the investigated section at the inside lane, as shown in Figure 10. Figure 11 shows the distress map of the investigated section. The DMI of longest longitudinal crack was observed between 860 and 1090.

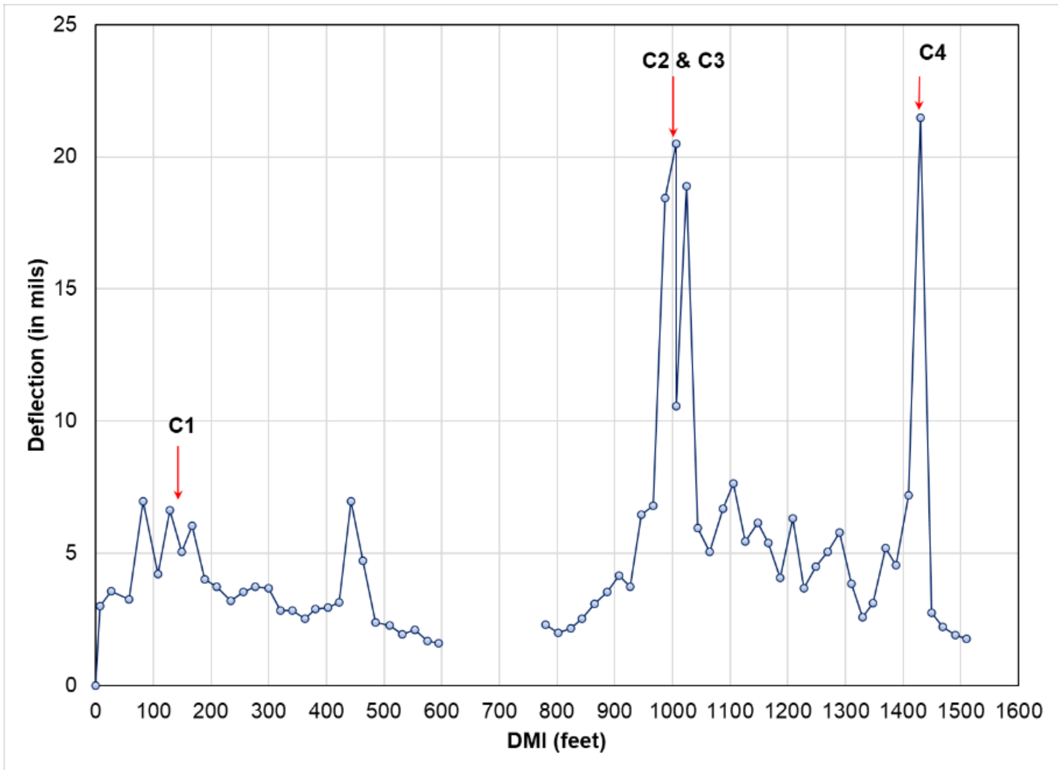

Figure 9 FWD deflections at the inside lane of the test section

Figure 10 Longitudinal crack observed between 940 and 1460 feet (DMI) in the inside lane

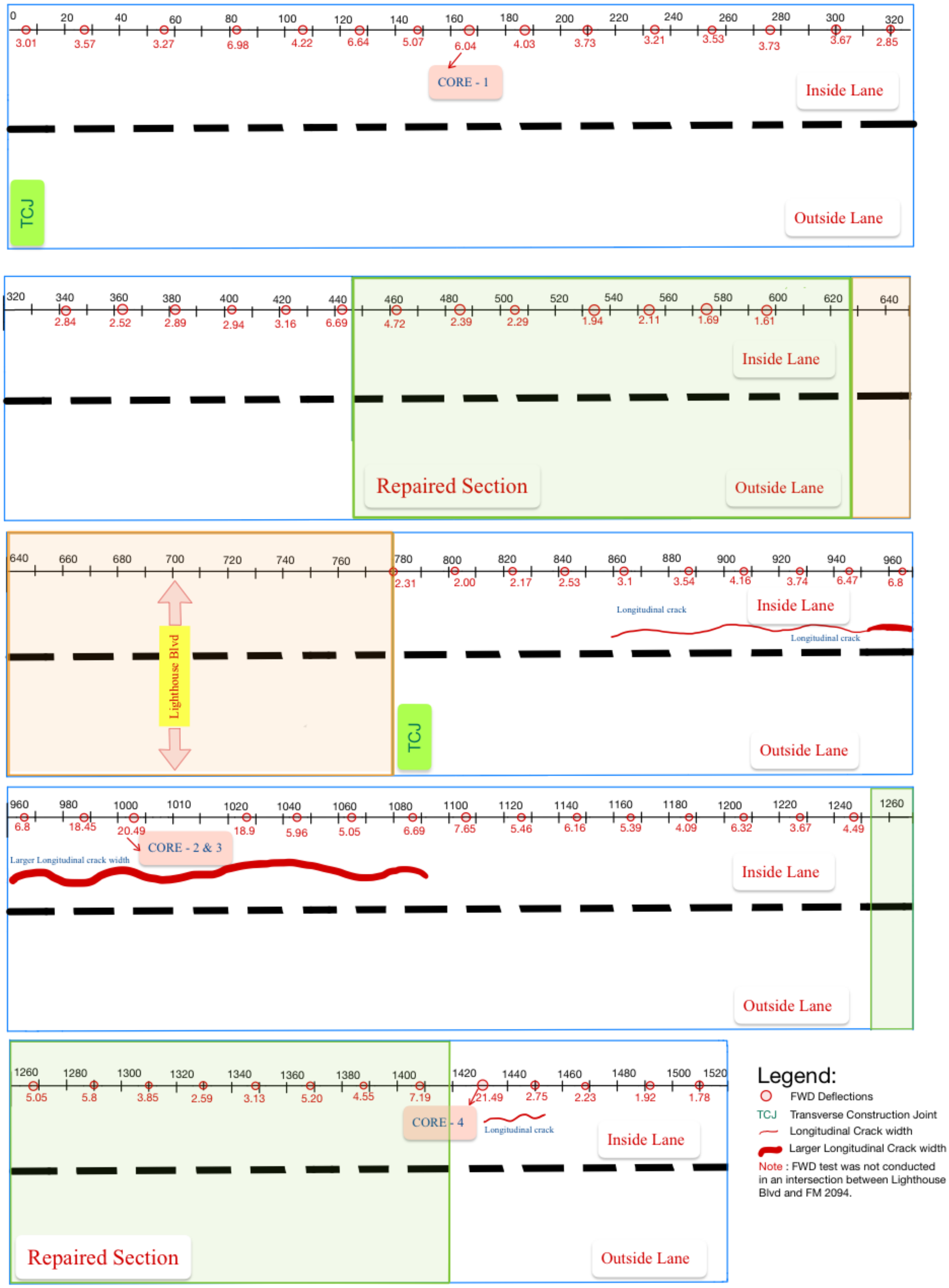

Figure 11 FWD deflection and distress map of the test section

Subgrade Modulus by DCP

The modulus of subgrade soil was estimated from DCP testing conducted at 4 coring locations. However, there was a technical issue during the DCP testing at the first location, which could have potentially compromised the dataset acquired; therefore, it was decided that it should be removed from the analysis. Figure 12 shows the DCP data on the other 3 locations. The slope of the DCP curves indicates the penetration rate per one blow, and the steeper slope indicates a larger penetration rate or lower modulus of soil. It can be observed that, at C3 and C4, the upper layer (up to 20-inches from the top of the subgrade layer) is less stiff compared to C2. In fact, the softer layer at C3 has continued until 35-inch depth. Figure 13 shows the modulus profile with respect to the depth at the three (3) locations. While C3 is at the same DMI as C2, C3 is located closer to the longitudinal joint as shown in Figure 14. Despite its proximity, the modulus profile is not similar and C2 is relatively stiffer. In addition, it was also observed that a large void (about 1.5-in) existed at C2 between the bottom of the concrete slab and asphalt bond breaker, as shown in Figure 15. This large void must have been developed due to differential volume changes. It is to be noted that uniform volume changes in the subgrade usually result in settlement of the slabs without large voids as observed here. Also, the large deflection at C2 (20.5 mils) must be due to this large void.

As a reference, Figures 16 show the subgrade modulus values obtained from DCP at locations in SS-5 project in front of University of Houston. It can be observed that the differences in modulus values are not large.

The information on slab deflections and subgrade modulus indicates that the structural capacity of this pavement system is adequate, after more than 30 years of service. The distresses observed in this project are not due to the deficiency of the pavement structural condition; rather, they are due to the volume changes in the subgrade. Accordingly, the selection of optimum rehabilitation options should consider the cause of the distresses observed here.

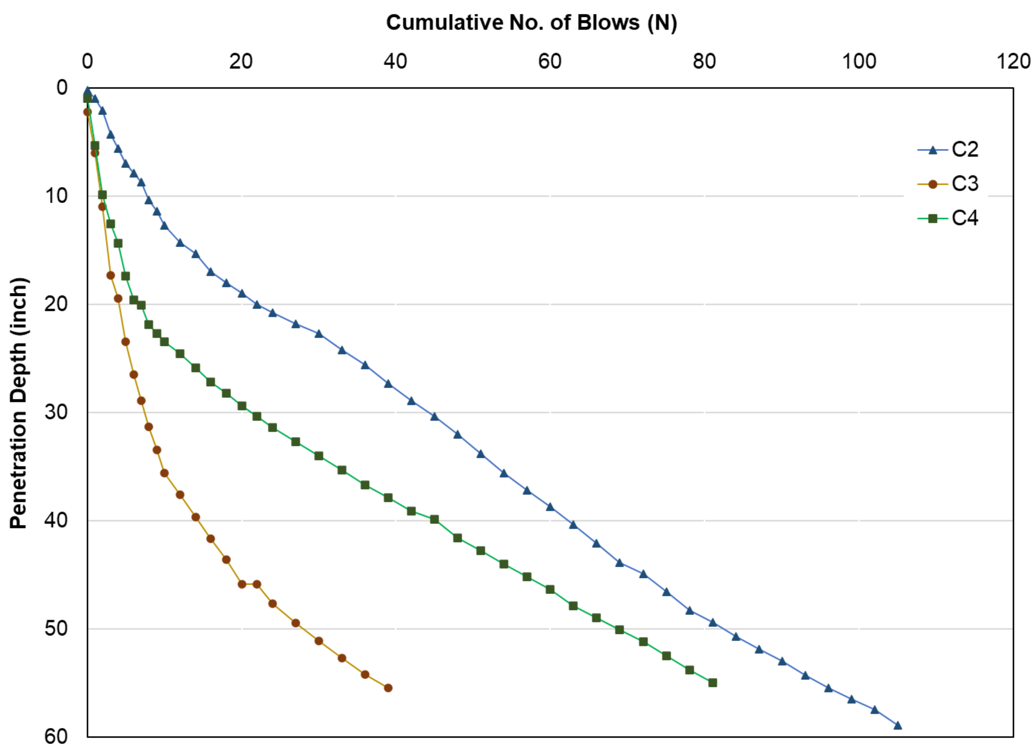

Figure 12 DCP data in the coring locations of the test section

<table>
<tr><th>Depth (in)</th><th>C2</th><th>C3</th><th>C4</th></tr>
<tr><td>1</td><td rowspan="11">8.19 ksi</td><td rowspan="35">4.27 ksi</td><td rowspan="23">5.94 ksi</td></tr>
<tr><td>2</td></tr>
<tr><td>3</td></tr>
<tr><td>4</td></tr>
<tr><td>5</td></tr>
<tr><td>6</td></tr>
<tr><td>7</td></tr>
<tr><td>8</td></tr>
<tr><td>9</td></tr>
<tr><td>10</td></tr>
<tr><td>11</td></tr>
<tr><td>12</td><td rowspan="49">15.8 ksi</td></tr>
<tr><td>13</td></tr>
<tr><td>14</td></tr>
<tr><td>15</td></tr>
<tr><td>16</td></tr>
<tr><td>17</td></tr>
<tr><td>18</td></tr>
<tr><td>19</td></tr>
<tr><td>20</td></tr>
<tr><td>21</td></tr>
<tr><td>22</td></tr>
<tr><td>23</td></tr>
<tr><td>24</td><td rowspan="37">17.44 ksi</td></tr>
<tr><td>25</td></tr>
<tr><td>26</td></tr>
<tr><td>27</td></tr>
<tr><td>28</td></tr>
<tr><td>29</td></tr>
<tr><td>30</td></tr>
<tr><td>31</td></tr>
<tr><td>32</td></tr>
<tr><td>33</td></tr>
<tr><td>34</td></tr>
<tr><td>35</td></tr>
<tr><td>36</td><td rowspan="25">13.02 ksi</td></tr>
<tr><td>37</td></tr>
<tr><td>38</td></tr>
<tr><td>39</td></tr>
<tr><td>40</td></tr>
<tr><td>41</td></tr>
<tr><td>42</td></tr>
<tr><td>43</td></tr>
<tr><td>44</td></tr>
<tr><td>45</td></tr>
<tr><td>46</td></tr>
<tr><td>47</td></tr>
<tr><td>48</td></tr>
<tr><td>49</td></tr>
<tr><td>50</td></tr>
<tr><td>51</td></tr>
<tr><td>52</td></tr>
<tr><td>53</td></tr>
<tr><td>54</td></tr>
<tr><td>55</td></tr>
<tr><td>56</td></tr>
<tr><td>57</td></tr>
<tr><td>58</td></tr>
<tr><td>59</td></tr>
<tr><td>60</td></tr>
</table>

Figure 13 Calculated modulus of the subgrade (Red: less than 5 ksi, Yellow: between 5 to 10 ksi, Green: over 10 ksi)

Figure 14 Proximity of C2 and C3 coring locations

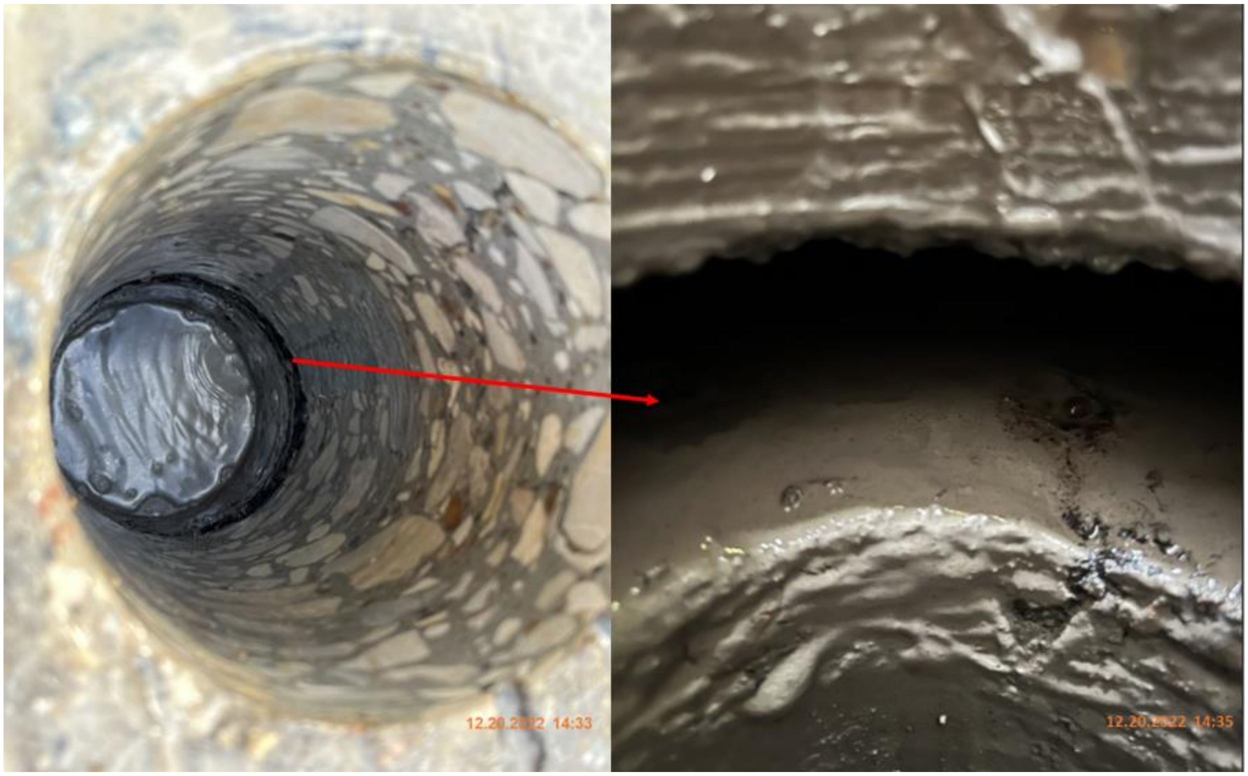

Figure 15 Cavity observed at C2

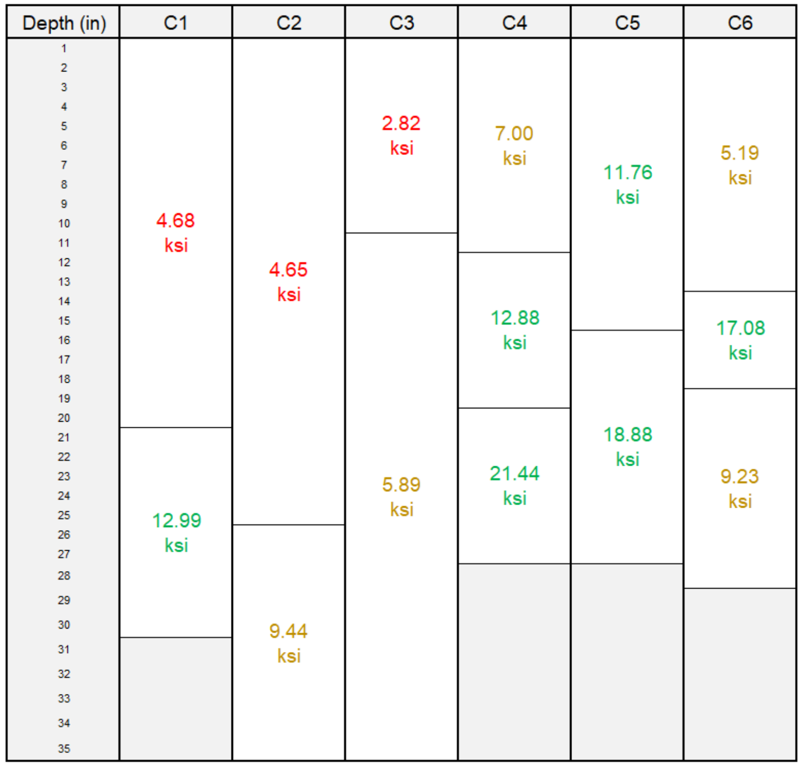

Figure 16 Modulus of subgrade soil from DCP in SS-5 in Houston

Subgrade Soil Characterization

Subgrade soil properties were evaluated in the laboratory. The soil properties evaluated were:

- Particle Size
- Atterberg Limits
- Shrink/Swell Potential

Heaving by the reactions between sulfate and lime was not considered as a potential cause for the distresses, as sulfate heaving has not been reported in the Houston area, and sulfate content was not evaluated.

The following testing procedures were followed:

- Tex-101-E Preparing soil and flexible base materials for testing
- Tex-103-E Determining moisture content in soil materials
- Tex-104-E Determining liquid limits of soils
- Tex-105-E Determining plastic limit of soils
- Tex-106-E Calculating the plasticity index of soils
- Tex-110-E Particle size analysis of soils
- Tex-142-E Laboratory Classification of Soils for Engineering Purposes
- The Shrink Swell Test (Fityus et al, 2005/ASTM)

No discussions are provided for the testing procedures since they are standardized testing, except for the shrink/swell testing.

<u>The Shrink Swell Testing (Fityus et al, 2005)</u>

There are no universally accepted tests for shrink/swell of subgrade soil – no ASTM or TxDOT test procedures available. In this investigation, the test procedure proposed by Fityus el al in 2005 was followed. Below described are the testing procedures followed:

Shrinkage Test: A shrinkage core of up to 2 inches in diameter and a length of 1.5-2 times the diameter as prepared from the collected soil sample. Figure 17 shows a shrinkage core specimen. The core specimen is prepared such that it is free of any defects or loose material. Initial dimensions and mass are recorded. Small pins are added to each end as reference points to facilitate consistent measurements of sample length as drying proceeds. The shrinkage core is first air-dried. Measurements of length and mass are recorded until shrinkage ceases. The core is then oven-dried to a constant mass of 221-230 ºF and final length and mass are recorded. The data recorded facilitates the calculation of the initial and final water contents and the axial strain.

Swelling Test: This involves a simplified oedometer test in which the sample is installed in a steel ring (usually around 2.5 inches in diameter and 1 inch high) and placed in a consolidation apparatus. An LVDT sensor is installed to monitor the sample height. A load of 3.6 psi (25 KPa) is then applied for 30 minutes to record any initial settlement or seating adjustment. This displacement is used to correct the initial sample height for the determination of the swelling strain. After re-zeroing the displacement gage, the sample is then inundated with distilled water and allowed to swell until the swelling increment in not more the 5% of the total recorded swell. The initial water content is determined from the sample trimmings and final water content is measured from the extracted soil sample at the end of the test. Figure

18 illustrates the sequence of the swell testing and Figure 19 shows the close-up view of the last phase of the swell testing.

Shrinkage and swell strains, measured in the respective tests, are then combined to give a shrink-swell index (I_{ss}). This is given by the following equation:

$$I_{ss} = \frac{\varepsilon_{sh} + \frac{\varepsilon_{sw}}{2}}{1.8}$$

where:
ε_{sh} is the shrinkage strain in %
ε_{sw} is the swelling strain in %

I_{ss} will be used to estimate ground surface movements, as will be discussed later.

Figure 17 Shrinkage core specimen

Figure 18 Swell testing procedure

Figure 19 Last phase of swell testing

Presentation of Testing Results

Soil Index Properties

Figure 20 shows the in-situ moisture content of the soil samples. It can be observed that another set of soil samples which were obtained from a CRCP project in Lubbock (PT1, PT2 and PT3) are included in the presentation of the results. In Lubbock, no undulations have been observed in CRCP, even when CRCP slab was placed directly on subgrade, which implies that the subgrade soil in this project has very little shrink/swell potential. As such, the test results of these soil samples will be used as comparison.

It is observed that, in general, moisture contents are quite high, which indicates that the soil is saturated during the time of testing, much larger than those in the soil in Lubbock. Moisture content in soil, especially clay, has a large impact on soil modulus, and an analysis was made to obtain the correlations between moisture content and soil modulus from DCP. Figure 21 presents the results (in red markers) along with the soil samples from SS-5, Houston (in blue markers). It can be observed that it shows strong correlations between moisture contents and soil modulus for both this and SS-5 projects. This dependency of soil modulus on moisture content is well established.

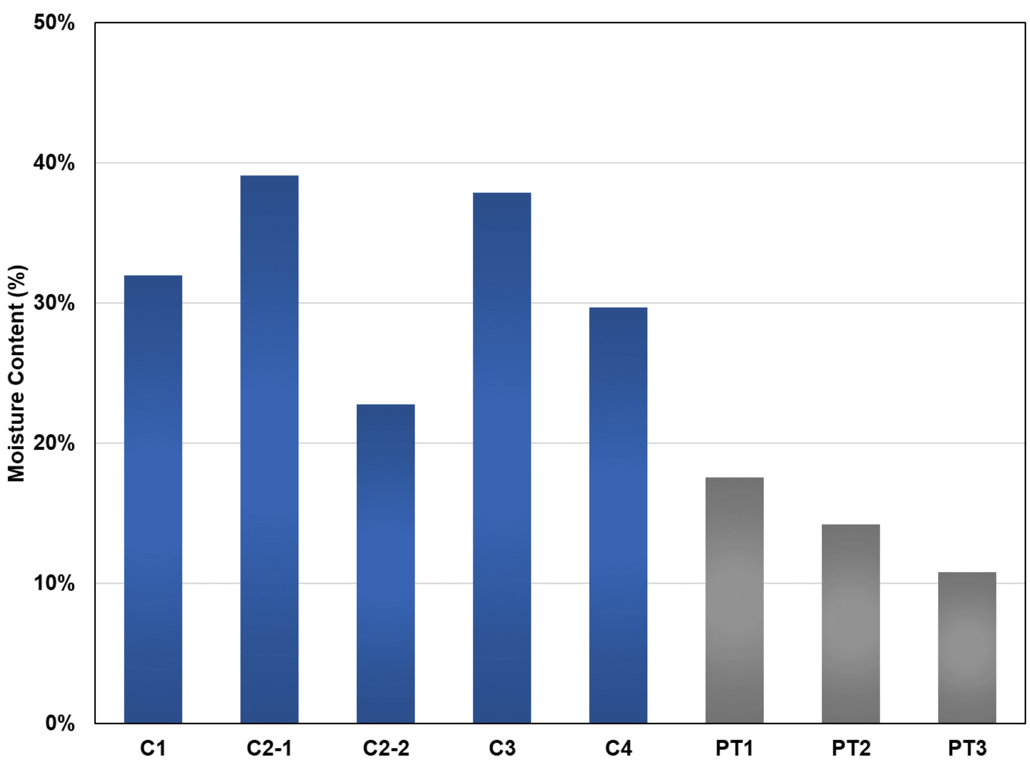

Figure 20 In-situ moisture content of the soil samples

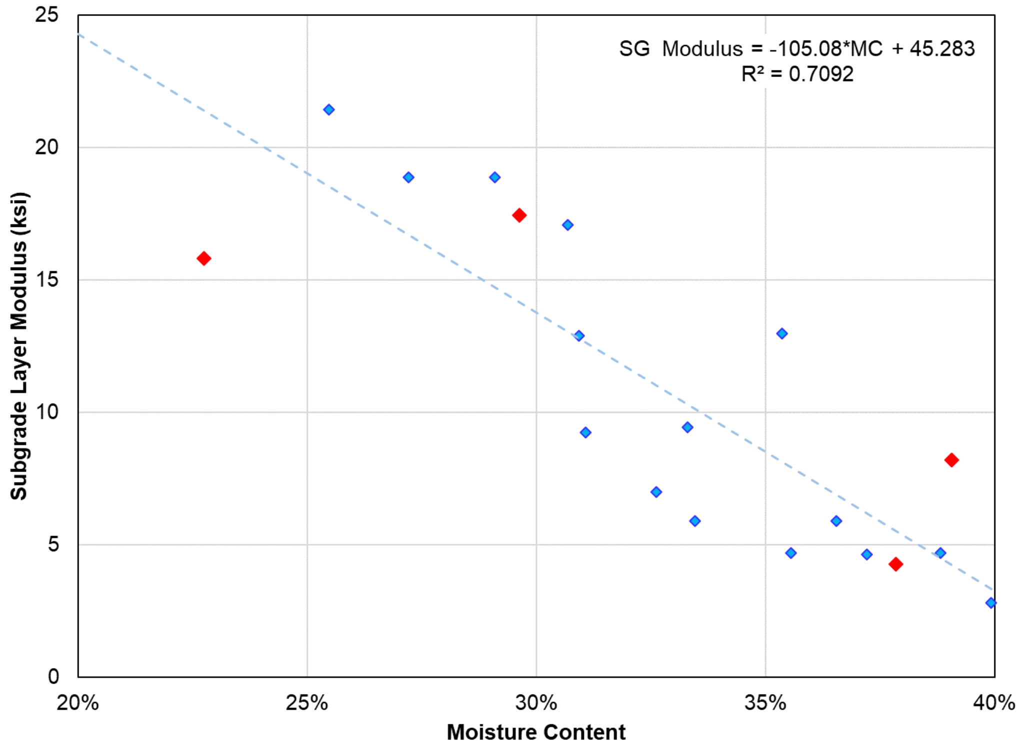

Figure 21 The relationship between in-situ moisture content and calculated subgrade modulus (red markers: FM 2094; blue markers: SS-5)

Figure 22 illustrates the gradations of soils from all 4 coring locations. Except for C1, the soil samples have particle sizes that are more than 50% finer than the 75μm (Sieve No. 200).

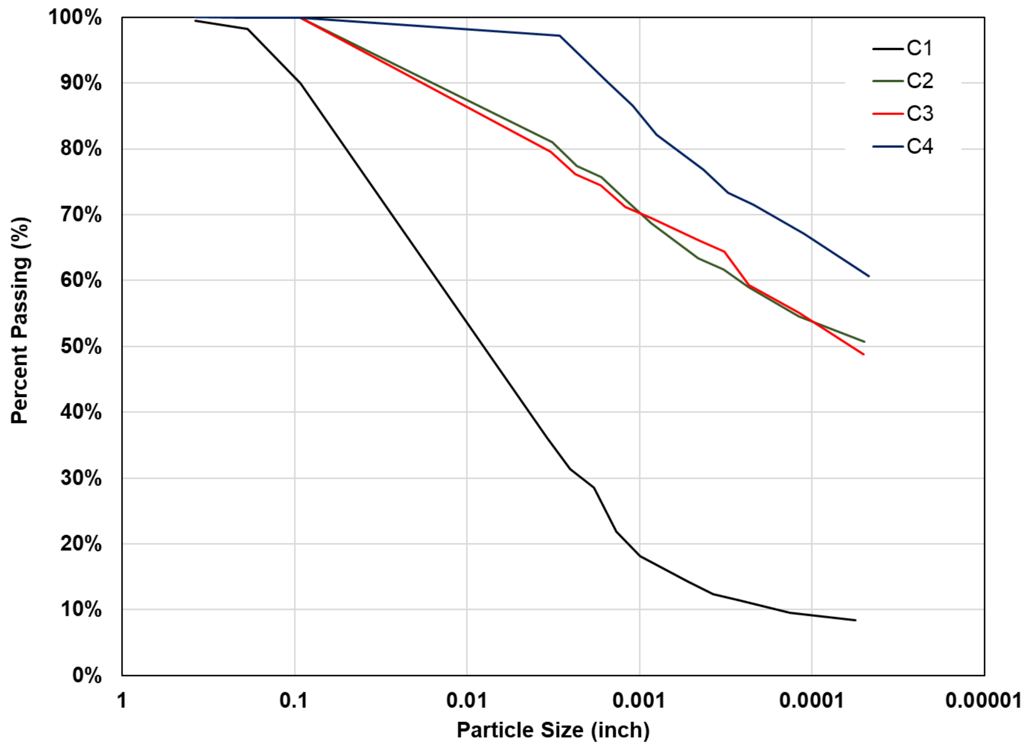

Figure 22 Particle size gradation in all coring locations within the test section

Figures 23 to 25 show the testing results of the Atterberg limits. Figure 26 shows that PI values are comparable to the Lubbock's soil samples. While PI values of the soil samples from Lubbock were slightly lower than those of the subject project's soil samples, the difference is not that significant.

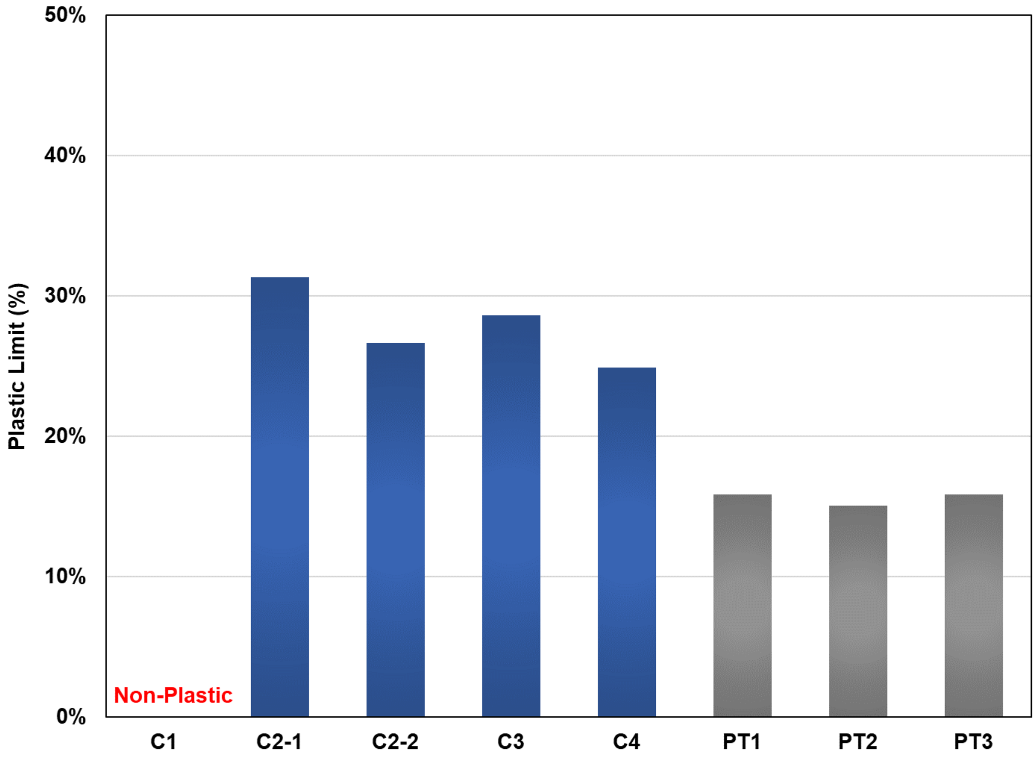

Figure 23 Plastic limit of soil samples

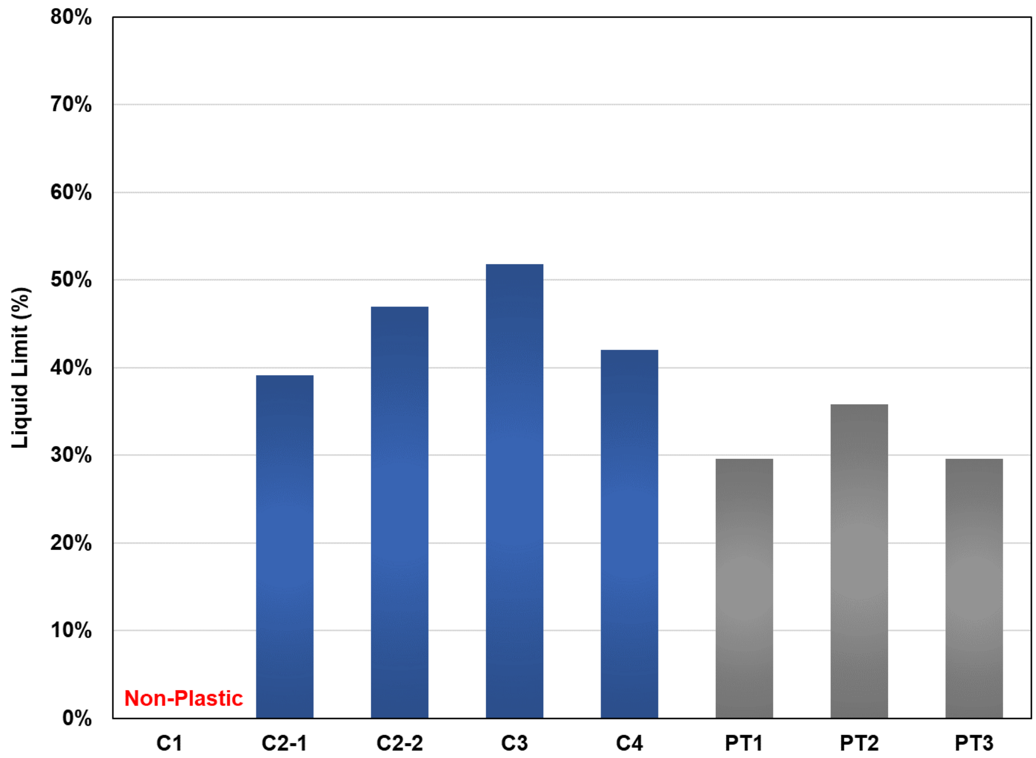

Figure 24 Liquid limit of soil samples

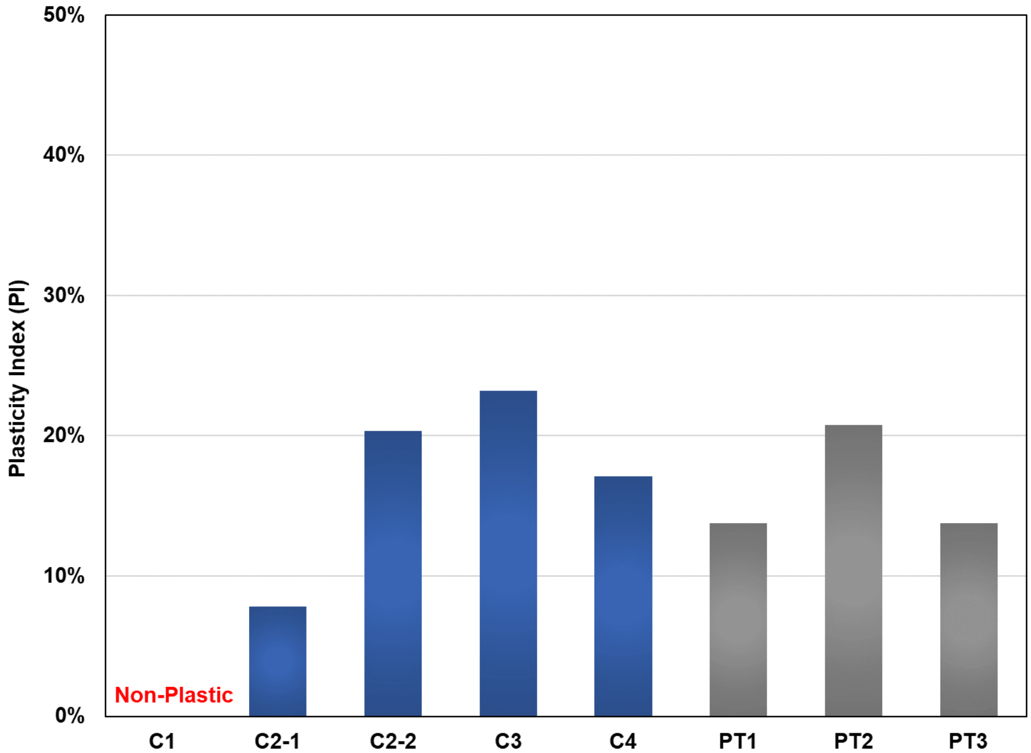

Figure 25 Plasticity index of the soil samples

Shrink Swell Test

Due to the insufficient amount of soil samples collected in C1, the shrink/swell test was not performed for that soil. Figure 26 shows that moisture contents increase after the swelling test. It is recalled that the soil sample is inundated with water during the swell testing. Moisture contents were determined before and after the swell testing. It can be observed that the moisture contents increased after being inundated with water and at 3.6 psi overburden pressure.

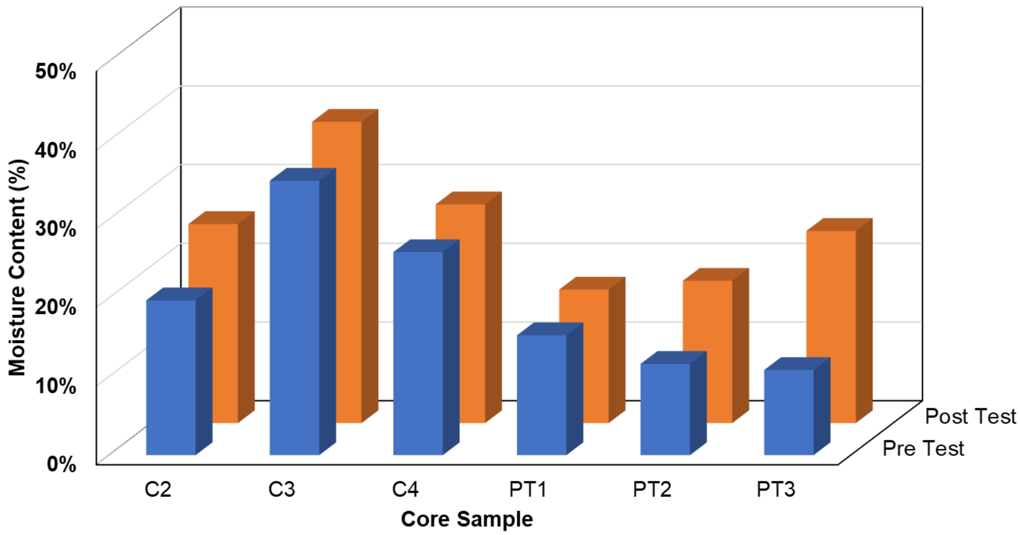

Figure 26 Moisture content before and after swelling test of soil samples.

Figure 27 shows the results of the swelling test. Time zero (0) represents the time when the soil specimen was inundated with water. It is recalled that the samples were under 3.6 psi compression. Since soil has compressive strength of roughly 10 psi plus/minus few psis, 3.6 psi pressure is not small. Still, all the soils from the subject project swelled even though the absorbed water during the testing was minimal. The soil at C2 has the highest swelling, about 22 mils which is almost twice as much as the highest swelling recorded in SS-5 project in Houston, where swelling varied from 3 mils to 11 mils. Meanwhile, C3 and C4 only swelled by 3 mils and 1 mil, respectively, as shown in Figure 28. Note that the proximity of the C2 and C3 is about 3-feet; however, the swelling potential is significantly different, which may indicate that the test section has a large variation of swelling potential. Meanwhile, 2 soil samples from Lubbock did not swell during the entire testing period, and one consolidated by 1 mil, by expelling voids under the 3.6 psi overburden pressure. Recall that the PI ranges between the subject project's soil samples and Lubbock's soil samples were comparable. However, it can be observed that the PI is not necessarily a good indicator of the swelling potential of the soil. This data clearly indicates the nature of the soil in the subject project as far as soil swell potential is concerned.

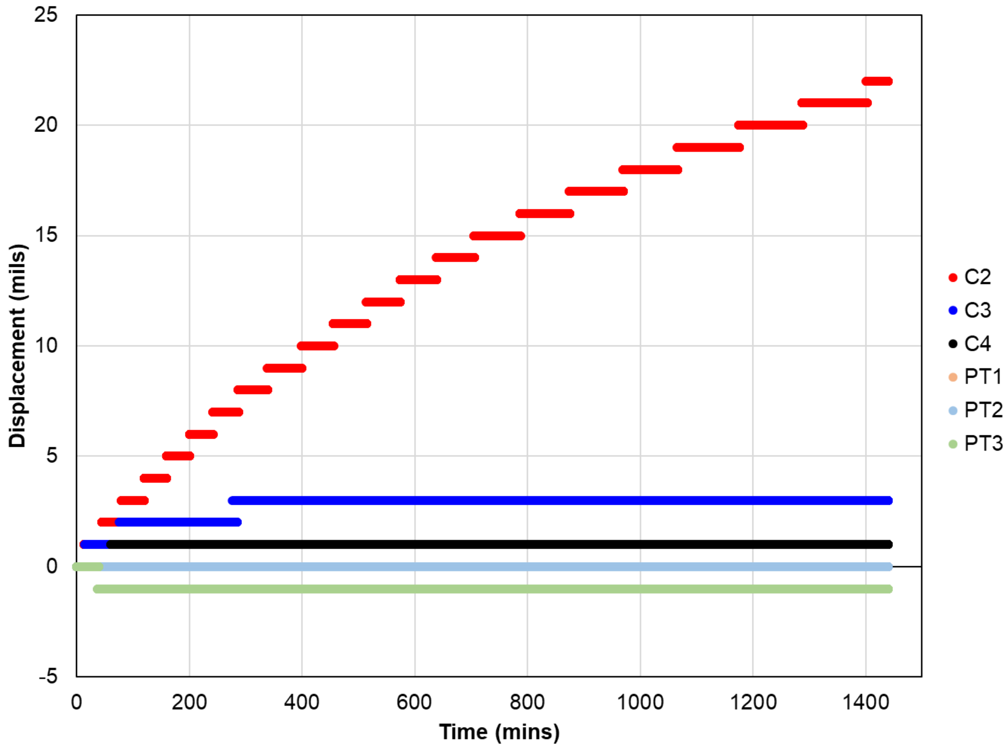

Figure 27 Swelling test results for soil samples

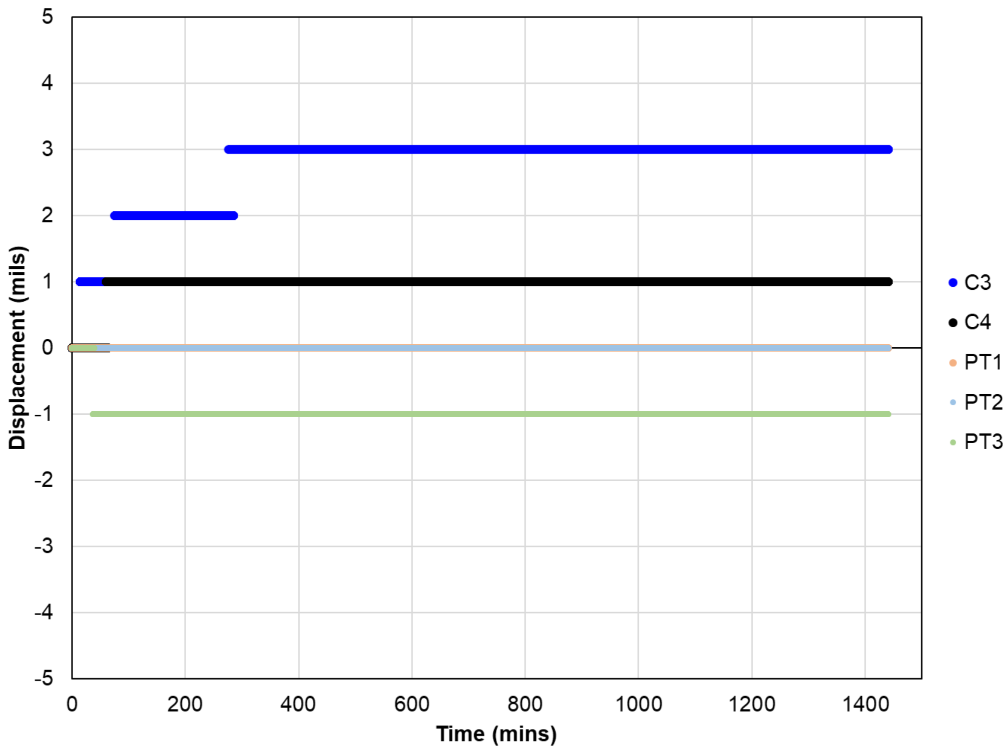

Figure 28 Swelling test results for C3 and C4 soil samples only

Table 1 below summarizes the swelling and moisture content variations between pre-test and post-test. It attempts to quantify the swelling potential per unit change in moisture content (1%). It is observed that one Lubbock soil sample lost water during the testing, and was consolidated, indicating that swell potential of this soil is almost zero. Meanwhile, for soil samples from the subject project, it is observed that moisture content increased during the swelling test. The rate of swelling per change in moisture is from 50 to 391 mils/(0.01*moisture change in %). Figure 29 presents the information in Table 1 in a graphical format. It clearly indicates that, compared with Lubbock soil, the soil in the subject project has much higher potential for swelling when absorbing moisture.

Table 1 Vertical rise and moisture content variation during swelling test

Soil Sample	**ΔMoisture Content (%)**	**Swelling, δ (mils)**	**Swell/ΔMC (mils/%)**
C2	5.63%	22	390.9
C3	3.42%	3	87.8
C4	2.00%	1	50.1
PT1	1.74%	0	0
PT2	6.48%	0	0
PT3	13.61%	-1	-7.3

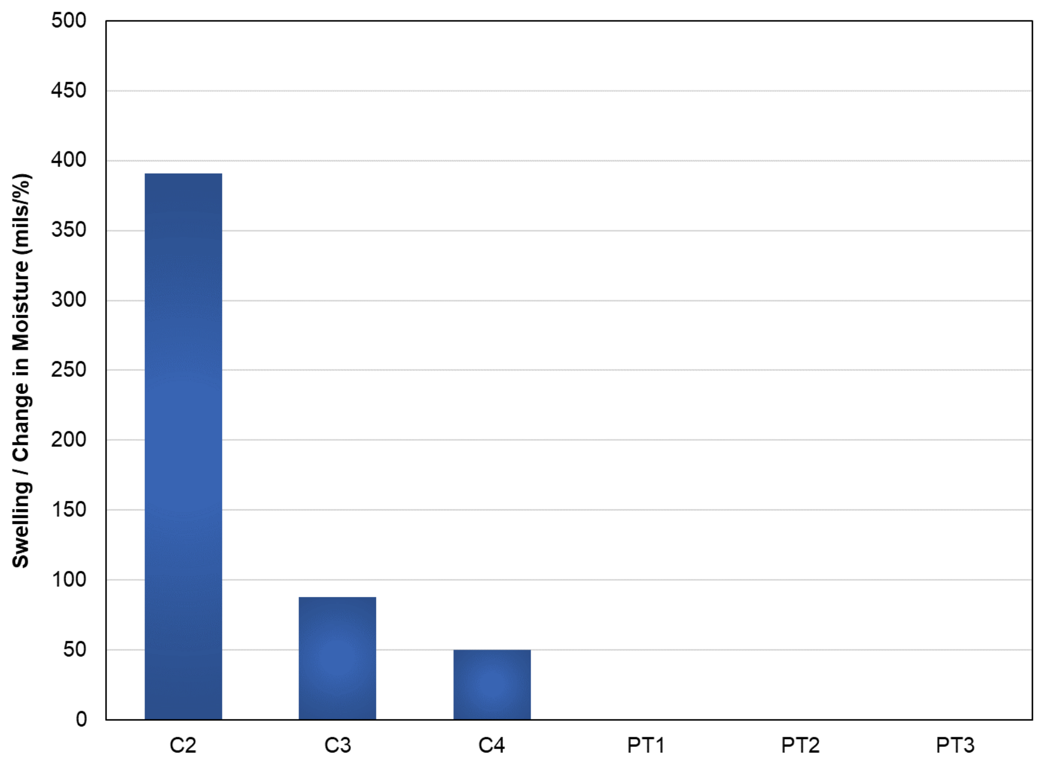

Figure 29 The rate of swelling per change in soil moisture in soil samples

Shrinkage testing consisted of measuring moisture contents as well as lengths of the soil samples at in-situ, air-dry and over-dry conditions. Figure 30 shows the moisture contents of soil samples at in-situ and air-dry conditions. The amount of moisture loss of the soils in the subject project is higher than the Lubbock's soil samples. However, the moisture loss in Lubbock soil samples were not translated into shrinkage, unlike the subject project's soil samples as shown in Figure 31. The shrinkage potential of the soils at the subject project is larger than that of the Lubbock's soil samples. This large shrinkage potential exacerbates the potential problems in the subject project. It could be concluded that the large shrinkage and swelling potential of the subgrade soil in the subject project is responsible for the pavement distresses observed.

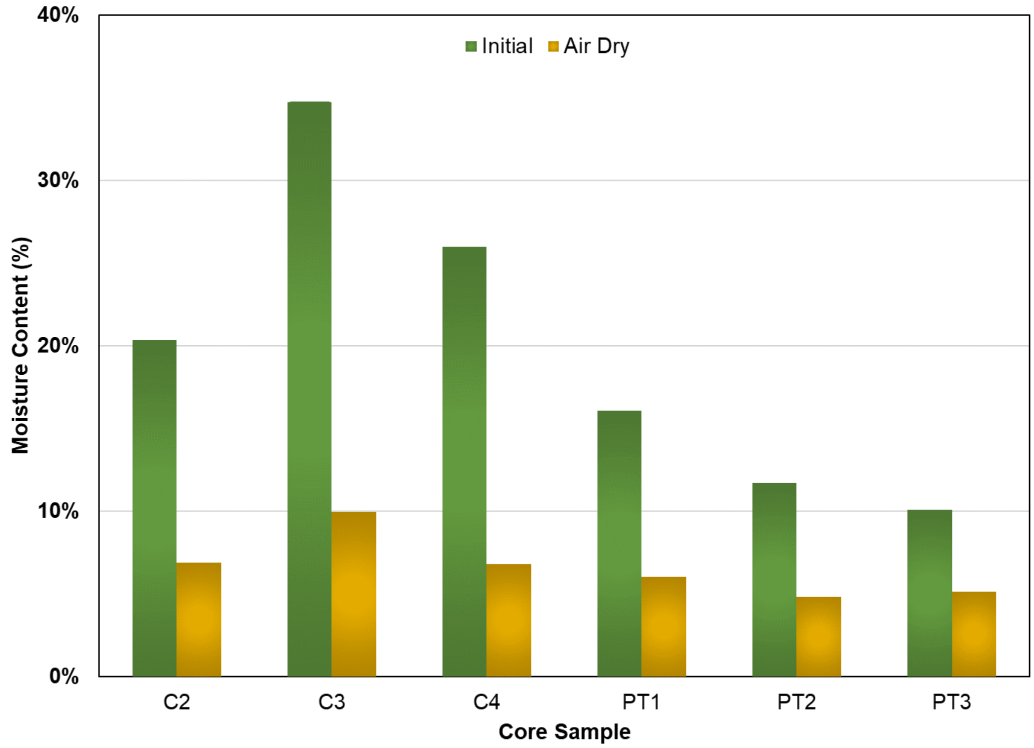

Figure 30 Shrinkage specimens' moisture content

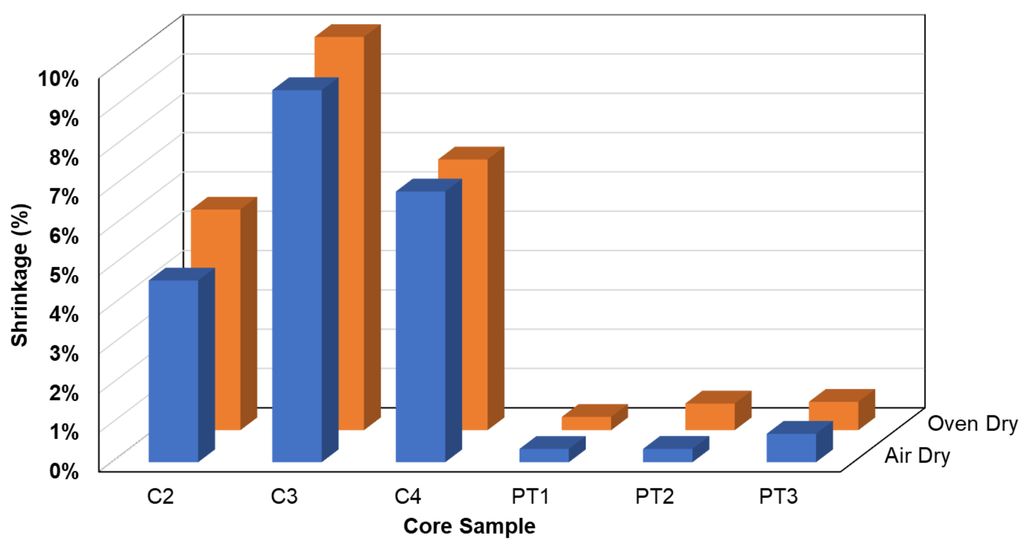

Figure 31 Shrinkage of soil samples after air dry and oven dry

Estimation of Ground Surface Movement

Fityus et al (2005) discussed that the shrink swell index gives a quantitative measure of the vertical strain that will occur in the soil per unit change of suction. Aitchison (1973) presented the following equation to estimate the net ground surface movement using the shrink swell index. In addition, the Australian Standard AS2870 uses the same equation to predict the characteristic surface movement that a particular soil may produce under seasonal moisture variations. The equation is given below:

$$y_s = \sum_{i=1}^{n} \propto \cdot I_{ss,i} \cdot \Delta pF_i \cdot \Delta z_i$$

where:
$I_{ss,i}$ is the shrink swell index of the soil layer
$\propto$= 2 constant multiplied to I_{ss} to account for the effects of lateral restraint
ΔpF_i is the magnitude of suction change assumed to be equal 1.8 pF units (6.3 KPa)
z is the layer depth

Figure 32 presents the net ground surface movements for soils from the subject project and Lubbock. It shows much larger ground surface movements potential in the subject project than in Lubbock.

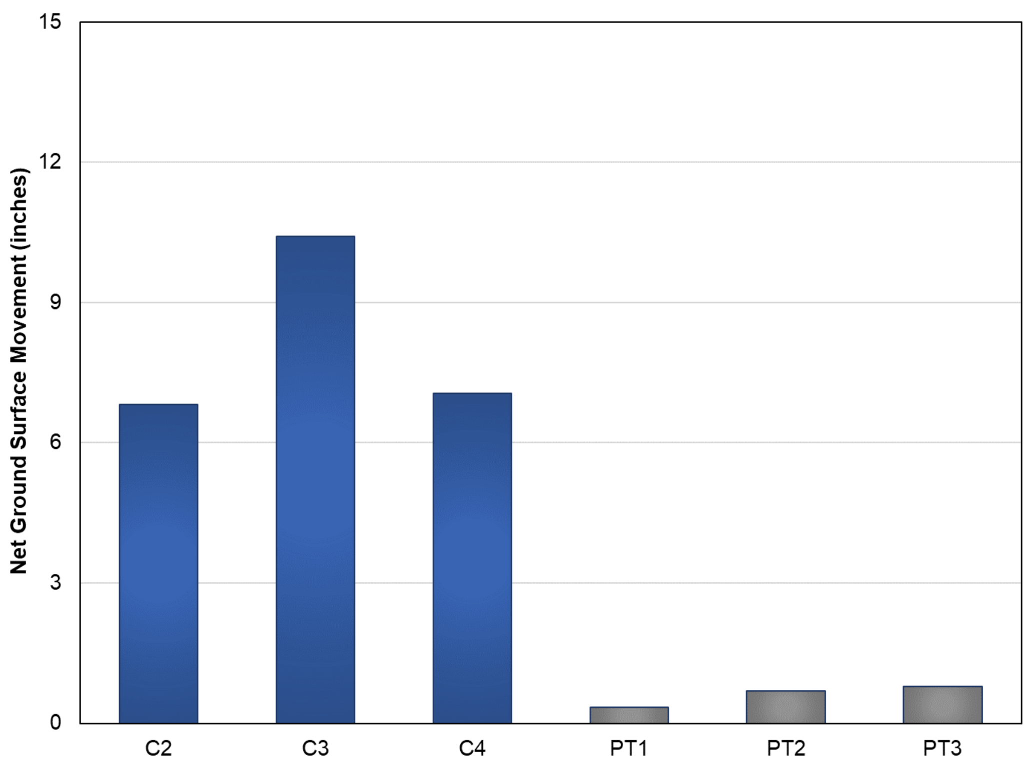

Figure 32 Characteristic soil movement of the soil samples

Summary

In this evaluation, pavement structural capacity was evaluated with FWD, while soil modulus, moisture contents/Atterberg limits, and volume change potential (shrink and swell) of the subgrade soil were evaluated with DCP and laboratory testing. The findings are summarized as follows:

- Subgrade soil in the subject project has much higher potential for shrink and swell during moisture variations than the soil in Lubbock. Also, a large variability was observed in swell potential among 3 locations evaluated in the subject project. This large shrink and swelling potential along with large variability is considered to be a major cause for the distresses observed in this project.
- Slab deflections in some areas are comparable to the state-wide average value for 10-in CRCP, while in other areas, the deflections are larger, which indicates voids under the slab. In general, except where voids exist, the structural capacity of the pavement system is adequate, especially considering the traffic being mostly passenger vehicles, without heavy trucks.
- In-situ moisture contents of the soil in the subject project are quite high, and soil modulus values evaluated by DCP are low.

It is concluded that the high volume change potential for the soil in the subject project was responsible for the distresses observed in the project – undulations of the pavement surface, faulting and uncontrolled cracking, especially longitudinal cracking.

Recommended Rehabilitation Options

Rehabilitation of pavement, including CRCP, where distresses are caused by soil volume changes, poses a real challenge. It is primarily because the difficulty in improving or modifying soil properties within a reasonable budget. Obviously, removing and replacing concrete slabs could fix the distresses and prolong the pavement service life for a while; however, since the practice does not eliminate the root cause of the problem, same type of distresses could develop. Removing concrete slabs and soil at some depths, followed by bringing in soil with low shrink and swell potential and placing new base and concrete slabs along with improving drainage system, might provide an ultimate solution. However, this practice could take a long time and could be quite costly, in addition to causing traffic disruptions in the well-established areas such as in the subject project.

An alternative would be the use of expandable polyurethane resin. This material has been used extensively to lift slabs and correct pavement undulations. The effectiveness of pavement repairs with this type of material has been mixed – some have performed well, while the same type of distresses developed again. Where the same type of distresses developed, it was not well established whether continued soil volume changes or degradations in the injected materials were responsible for the recurrence of the distresses.

The vertical compressive stress at the bottom of the 10-in slab due to the slab weight or 9,000-lb wheel loading is about 1 psi, respectively. This stress value is quite small. Also, the traffic in the subject project is mostly cars and pick-up trucks, with very few heavy trucks. Accordingly, the degradation of the injected materials due to large stresses is not likely, considering the compressive strengths of the injected materials vary from 80 psi to 110 psi for 4 lb/cf and 5 lb/cf of densities, respectively. Degradation due to chemical reactions has not been reported.

Considering the nature of the distresses and traffic characteristics in the subject project, it is recommended that the undulations or faulting are repaired by expandable polyurethane resin. How long this repair will stay effective will depend on the continued soil volume changes in the project site. However, it is considered that the performance of this repair might be comparable to full-depth repairs with Item 361, with a lower cost, since this material costs about $5 per pound.

To further improve the repair performance with this method by reducing the potential for soil shrink and swell, the same material (expandable polyurethane resin) can be injected into soil. A comprehensive review of the performance of soil treated by this material indicates good performance (Sabri, et al, 2021). The use of the soil treatment with this material might be tried at some portions of the project, and its performance could be evaluated and compared with the control section (no treated area). The data to be obtained in this trial could provide valuable information for TxDOT and others, since this type of distresses are not uncommon.

References

Fityus, S.G. (2005), Cameron, D.A., and Walsh, P.F. *The shrink swell test*, Geotech Test J, 28, pp. 92-101

Atchison, G.D. (1973), *Quantitative Description of Stress-Deformation Behavior of Expansive Soil*, Proceedings of the 3rd International Conference on Expansive Soils, Haifa, Vol 2, pp. 79-82

AS 2870-1996: Australian Standard: Residential Slabs and Footings, Standards Australia.

Sabri, M., Vatin, N., and Alsaffar, K. (2021), *Soil Injection Technology Using an Expandable Polyurethane Resin: A Review*, Polymers, 13, 3666